AIPS Memo 86

Widefield Polarization Correction of VLA Snapshot Images at 1.4 GHz

W. D. Cotton

National Radio Astronomy Observatory, Charlottesville, VA

16 March, 1994

Abstract

This memo describes measurments of the off–axis polarization pattern of the VLA antennas at frequencies near 1.4 GHz and techniques for correcting these effects in snapshot images.

1 Introduction

Napier 1989 has shown that the instrumental polarization response will vary across the primary beam of the antenna pattern; the determination and removal of this effect is necessary for accurate, widefield polarization imaging. This memo describes efforts made to this end as part of the VLA D array sky survey. The antenna polarization pattern was only measured at selected frequencies near 1.4 GHz and corrections only applied to snapshot observations but the same techniques could be used at other frequencies and adapted to extended synthesis observations. These corrections apply only to linear polarization; corrections for circular polarization are signifigantly more difficult.

2 On–axis Polarization Calibration

The standard practice for calibrating linear polarization data from with the VLA (Fomalont and Perley 1989), as with other synthesis arrays, is to determine the spurious instrumental response to an unpolarized signal from a calibrator source on the axis of the antenna pattern in terms of the "leakage" (or "D–term") model. The on–axis instrumental polarization is then removed from all data by subtracting the spurious instrumental response determined from the antenna "D–terms" and the measured total intensity. The effects of the parallactic angle (apparent rotation of the feed as seen by the source) are removed from the corrected data by rotating the phase of the observed cross-polarized visibilities by plus or minus (LR or RL correlations) the sum of the parallactic angles of the antennas. This rotation by the sum of the parallactic angles corrects the response to the source polarization but will cause any residual spurious instrumental response to display a polarization angle that rotates with parallactic angle. Because the instrumental polarization response varies with location in the antenna pattern this procedure is adequate only near the axis of the antenna pattern.

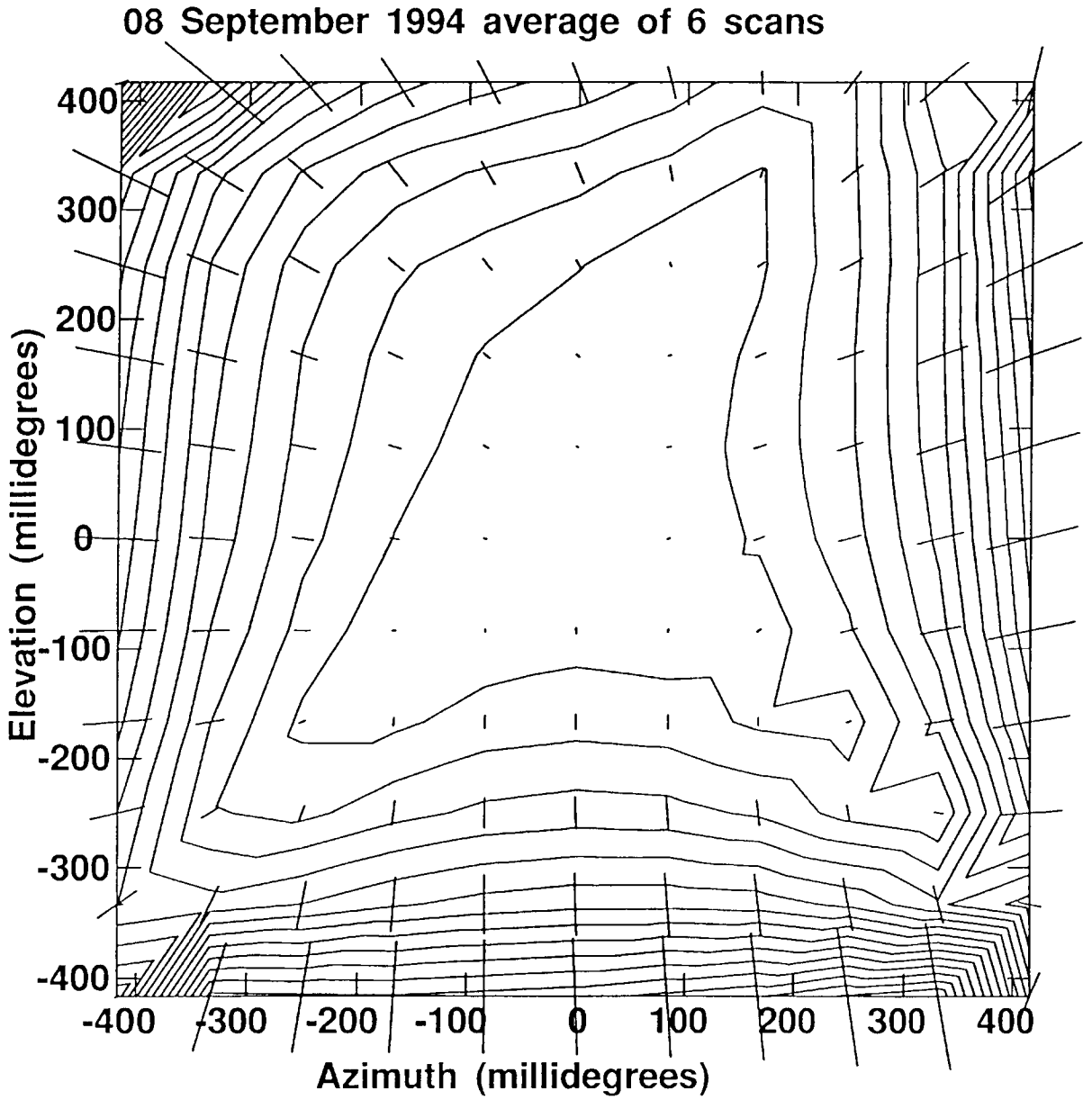

Figure 1: The off-axis instrumental polarization derived from 6 sources on 08 September 1993. The contours are every percent of instrumental polarization; the vectors have lengths proportional to the instrumental polarization and orientations of the instrumental polarization. Two 50 MHz bands are averaged. The individual scans in this composite were indistinguishable.

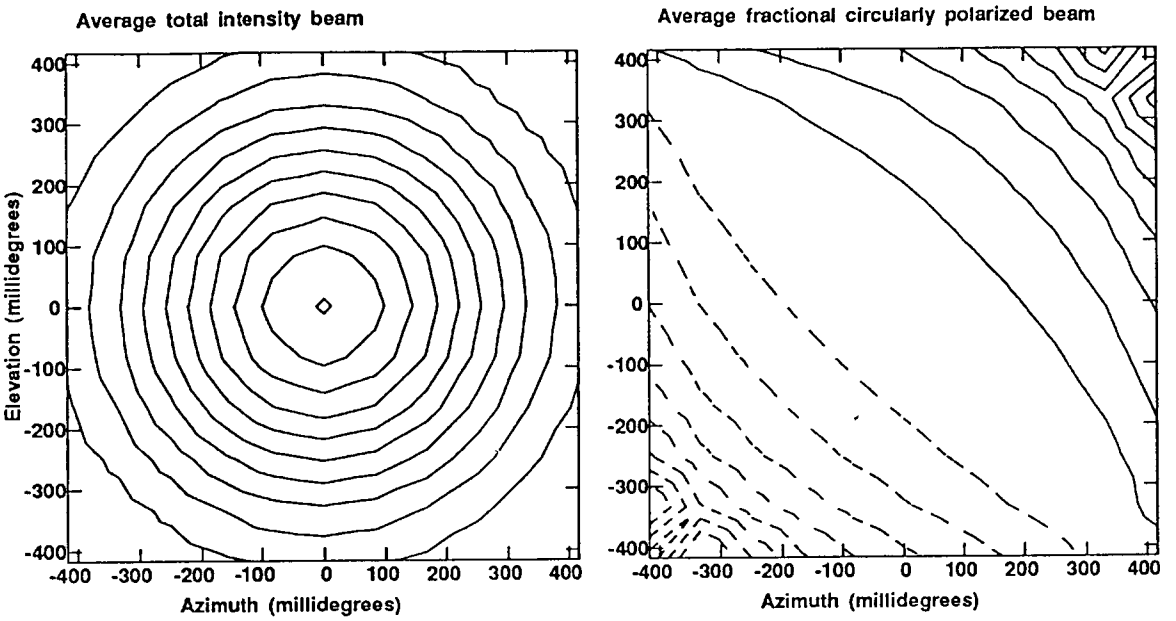

Figure 2: Left: The normalized total intensity response of the VLA antennas derived from 6 sources. The contours are every 10 percent.
Right: The fractional circularly polarized response of the VLA antennas as Stokes' V derived from 6 scans. The left– and right–handed responses were normalized at zero offset by the standard calibration process. The contours are every 5 percent; dashed contours are negative.

3 VLA Residual Antenna Polarization Pattern

In order to explore the off–axis polarization pattern, observations of the regions around bright sources were made in modified holography mode and gridded into an image of the antenna pattern in Stokes' I, Q, U, and V. The details of this process are given in a later section. A representation of the fractional linear polarization beam derived from several sources is shown in Figure 1. These observations were made at a variety of observing geometries and with a mixture of polarized and unpolarized sources and are consistent at the level of uncertainty of the individual source measurments. This pattern therefore appeared to be stable with observing geometry at a single epoch. For reference, the total intensity and circular polarization antenna patterns are shown in Figure 2.

3.1 Frequency Effects

The data shown in Figure 1 are the average of two 50 MHz bandpasses centered at 1.365 and 1.435 GHz and therefore refer to an average frequency of 1.4 GHz. The pattern shown in Figure 1 varies quite strongly with observing frequency. The linear polarization patterns in the individual 50 MHz bands are compared in Figure 3. It therefore appears that the beam polarization characteristics must be determined for each frequency configuration to

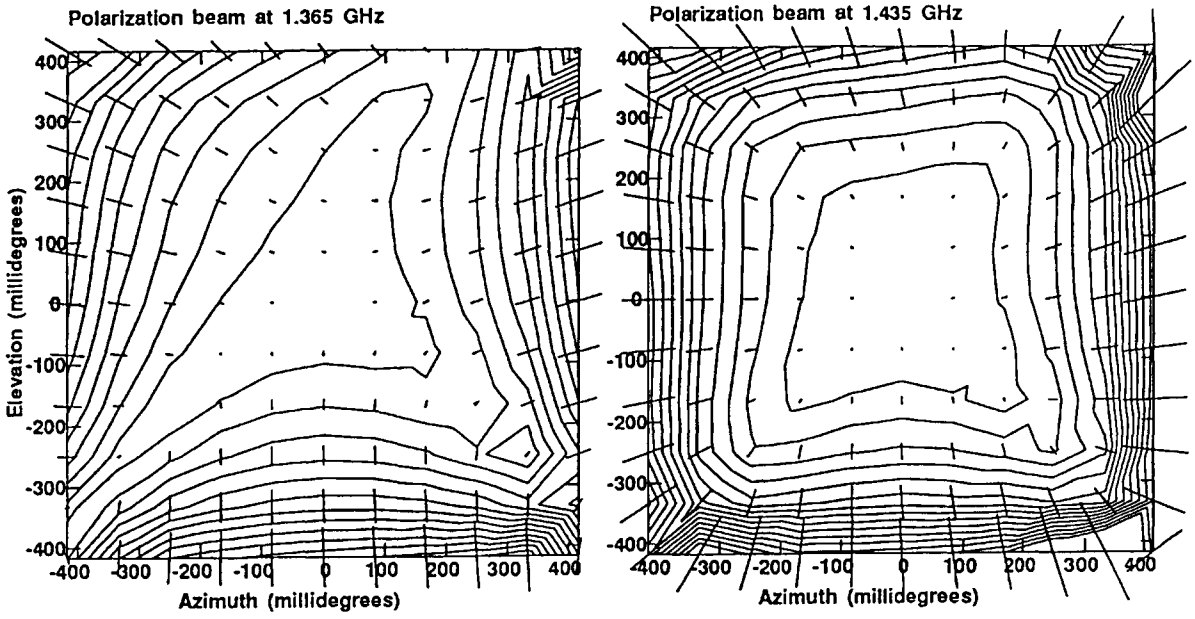

Figure 3: The off–axis instrumental polarization in the two 50 MHz bands used. Signifigant differences are apparent over the 70 MHz separation in the two frequencies

be corrected.

3.2 Stability in Time

If the off–axis instrumental polarization is determined primarily by the antenna configuration then it should be relatively stable in time. This expectation is confirmed in Figure 4 as well as in tests of the correction process described later. The data shown in Figure 4 were obtained using the same frequencies and techniques as those in Figure 1 but on a different source and approximately four months later. Excluding the outer two rows in the images shown in Figures 1 and 4 the average and RMS of the difference is 0.1%. This comparison includes all regions with an antenna gain above 30%. The amplitude of the difference of the polarization patterns is also shown in Figure 4. Much of the difference seen at high negative azimuth offsets is due to strong interference during these observations requiring heavy editing of one of the two 50 MHz bands.

4 Measurment of the Antenna Polarization Pattern

The antenna polarization pattern was determined using a modification of the holography mode of the VLA control system. The major modification was that all antennas were moved to the same off-source position rather than leaving "reference" antennas pointing on-source. Thus, the polarized power pattern rather than the voltage pattern was measured. Prior to being gridded the data are fully amplitude, phase and on–axis polarization calibrated and converted to i, q, u and v. The data for each offset are time and frequency averaged and

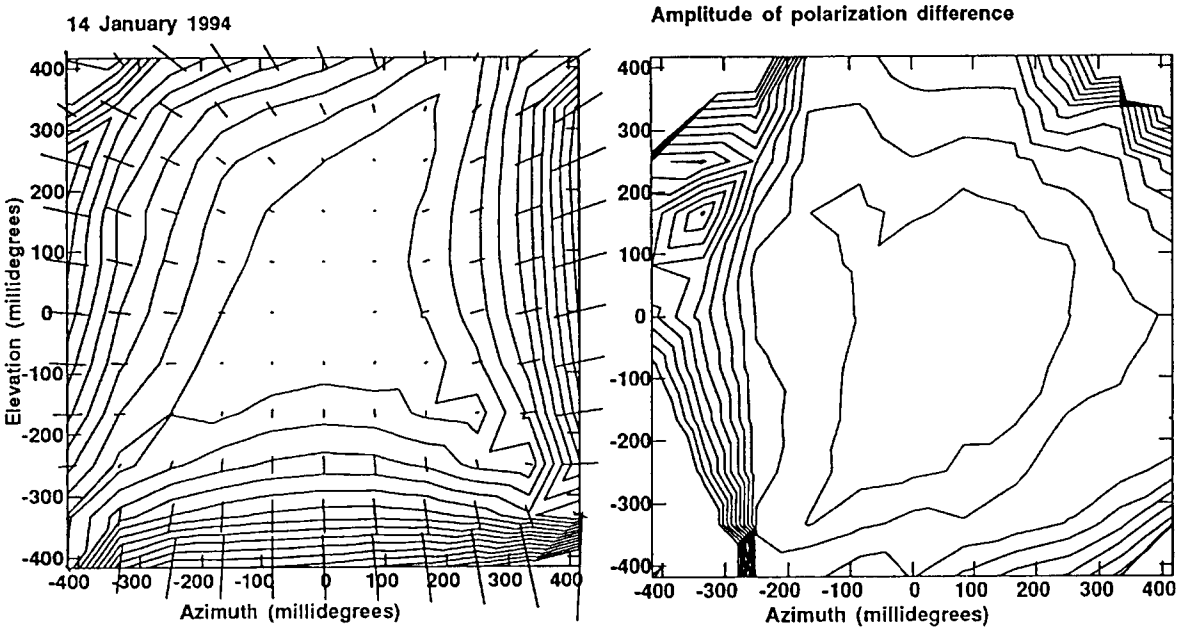

Figure 4: Left: The off–axis instrumental polarization derived from a single scan on a single source on 14 January 1994 shown as in Figure 1. This is the average of two 50 MHz bands. Right: The amplitude of the difference between the polarization image shown above with that in Figure 1. The innermost contour is at 0.5% and the rest are every percent. See text for an explanation of the values at high negative azimuth offset.

atmospheric phase effects are removed and the values converted to fractional polarization by dividing the polarized responses by the "i" correlation and then averaged over baseline. A correction for the expected "q" and "u" correlations due to the measured polarization of the source is then applied. Finally, the erroneous effects of the on–axis polarization calibration must be undone by rotating (q + ju) by minus the sum the parallactic angles of the antennas.

The images shown in this memo are 11 × 11 rasters with 5 arcminute spacings in azimuth and elevation. The actual rasters are made in true azimuth and elevation offset but the beam images need to be projected onto a plane whose tangent point is at zero offset. For holography mode data, AIPS task FILLM (which reads the VLA archive tapes) returns the projected azimuth and elevation offsets as the "u" and "v" coordinates attached to the measured visibilities. Since the observations are not made on the grid being used for the image, the observations must be interpolated onto the grid. This process in incorporated into the AIPS task MAPBM.

The transformation from azimuth and elevation to the projected coordinates is given by the following (M. Kestevan private communication):

$$u = -cos(E)sin(A - A_0)$$

$$v = -cos(E)sin(E_0)cos(A - A_0) + sin(E)cos(E_0)$$

where E is the elevation of a given pointing, E_0 the elevation of the source, A is the azimuth of the pointing and A_0 the azimuth of the source.

5 Correction of Snapshot Images

The beam polarization images derived by the procedure above are of fractional polarization and the spurious instrumental response as a function of sky position is the product of this complex, fractional polarization image and the total intensity image of the source. However, there are two effects of the observing geometry that complicate this correction.

The first effect is that the instrumental polarization pattern is fixed to the antenna and therefore rotates on the sky as the antenna tracks the source. For a snapshot observation this rotation (parallactic angle) can be considered constant and the antenna polarization image can be rotated to the orientation of the observation by a rotation in the plane of the sky. The amount of this rotation is the parallactic angle of the observation.

The second effect is that the standard on-axis polarization calibration will have rotated the polarization vector of the instrumental polarization by minus the sum of the parallactic angles to remove the effects of parallactic angle from the source polarization. This effect can be removed by rotation the instrumental polarization image by plus the sum of the parallactic angle in the Q-U plane.

As both of these effects vary with the observing parallactic angle and hence with time, this correction is only straightforward for a snapshot observation where the parallactic angle can be considered constant. For a snapshot image, the off-axis instrumental polarization can be applied by making the two rotations described above to the beam polarization image, multiplying the result times the total intensity image and subtracting from the observed source polarization image.

The correction of snapshot images is implemented in AIPS task VLABP. As part of the testing of the calibration for the VLA D array survey, a number of observations were made of strong sources with various pointing offsets. These observations were processed in the same manner as normal survey observations including widefield polarization corrections using task VLABP. The calibration images were those shown in Figure 1 and were made from observations obtained in early September 1993. The test observations were made in January 1994; the results of these tests are given in Table 1. This table gives the offset in Right Ascension and Declination, the parallactic angle of the observation, and the antenna gain. The final two columns give the amplitude of the residual instrumental polarization without ("uncorrected") and with ("corrected") off-axis polarization calibration expressed as a percentage of the total intensity. The source used (3C295) was unpolarized so no correction was needed for source polarization.

The measurments given in Table 1 are clustered at a number of levels in the primary beam. The typical antenna gain, the number of measurments and the average and worst cases for each of these clusters are given in Table 2 for images without ("raw") and with ("corr.") off-axis polarization calibration. As in Table 1 the values are the amplitude residual instrumental polarization expressed as a percentage of the total intensity. Widefield polarization calibration appears to reduce the instrumental polarization typically by a factor of 3 – 5.

6 Conclusions

The effects of off-axis instrumental polarization can be a serious problem when widefield polarization observations are made. The uncorrected residual instrumental polarization can be several percent in regions of signifigant antenna gain. Routines MAPBM and VLABP have been implemented in the AIPS image processing system which can make beam polarization images from quasi-holography mode observations and apply these corrections to widefield snapshot images. This correction appears to reduce the instrumental polarization by factors of 3 to 5 over regions of interest in the primary beam. In the tests presented here, the residual instrumental polarization after full beam correction did not exceed 0.5% within the half power of the primary antenna pattern.

Acknowledgements

I would like to thank Mike Kestevan and Ken Sowinski for their help in understanding the holography mode of the VLA and Mark Holdaway for discussions on antenna beam polarization

References

Fomalont, E. B. and Perley, R. A. 1989, in *Synthesis Imaging in Radio Astronomy*, ed. R. A. Perley, F. R. Schwab, and A. H. Bridle (San Francisco: Astronomical Society of the Pacific), p. 83.

Napier, P. J. 1989, in *Synthesis Imaging in Radio Astronomy*, ed. R. A. Perley, F. R. Schwab, and A. H. Bridle (San Francisco: Astronomical Society of the Pacific), p. 39.

Table 1: Measurments of Sources

Δ RA [']	Δ Dec [']	Parallactic angle [Deg]	gain	Uncorrected[%]	Corrected [%]
0	0	180	1.00	0.02	0.03
0	5	156	0.91	0.39	0.05
0	10	155	0.74	0.68	0.22
0	15	155	0.51	1.22	0.25
0	20	154	0.28	2.37	0.27
0	25	154	0.12	4.34	0.78
0	-5	153	0.92	0.36	0.13
0	-10	152	0.74	1.00	0.21
0	-15	151	0.51	1.98	0.37
0	-20	151	0.28	3.70	0.66
0	-25	150	0.12	6.66	1.48
0	0	-159	1.000	0.03	0.03
5	0	-152	0.93	0.13	0.15
10	0	-152	0.77	0.09	0.21
15	0	-153	0.53	0.09	0.23
20	0	-154	0.29	0.57	0.17
25	0	-155	0.12	1.69	0.45
-5	0	-154	0.92	0.32	0.14
-10	0	-155	0.75	1.02	0.30
-15	0	-155	0.51	2.38	0.49
-20	0	-156	0.28	4.74	0.80
-25	0	-156	0.03	20.2	
0	5	-157	0.91	0.40	0.01
0	10	-158	0.75	1.12	0.18
0	15	-158	0.51	2.38	0.36
0	20	-158	0.28	4.50	0.61
0	25	-158	0.11	7.70	1.20
0	-5	-160	0.93	0.14	0.12
0	-10	-162	0.76	0.57	0.17
0	-15	-163	0.52	1.58	0.36
0	-20	-164	0.30	3.96	0.96
0	-25	-165	0.12	7.52	1.90
7	7	-164	0.86	0.47	0.13
14	14	-164	0.56	1.33	0.39
21	21	-165	0.24	3.17	1.08
-7	7	-166	0.86	0.04	0.08
-14	14	-166	0.55	0.43	0.07
-21	21	-166	0.23	1.72	0.13
7	-7	-169	0.86	0.44	0.17
14	-14	-170	0.58	1.47	0.36
21	-21	-171	0.26	3.48	0.69
-7	-7	-170	0.86	0.45	0.17
-14	-14	-171	0.57	1.30	0.20
-21	-21	-172	0.24	2.90	0.53

Table 2: Summary of Corrections

Gain	Number	avg. raw[%]	max. raw[%]	avg. corr.[%]	max. corr.[%]
0.90	10	0.31	0.47	0.12	0.17
0.75	6	0.75	1.12	0.22	0.30
0.50	10	1.42	2.38	0.31	0.49
0.25	10	3.10	4.74	0.59	1.08
0.12	5	5.58	7.70	1.16	1.90